Mol Cell Biochem (2011) 351:207–215
DOI 10.1007/s11010-011-0728-2

Interaction of microtubules and actin with the N-terminus of βPix-b_L directs cellular pinocytosis

Seung Joon Lee · Soo Jung Yang · Dae Hwan Kim · Jhang Ho Pak · Kwang Ho Lee · Kyoung Hee Choi · Dongeun Park · Sangmyung Rhee

Received: 24 August 2010 / Accepted: 10 January 2011 / Published online: 20 January 2011

Abstract βPix is a Rac/Cdc42 guanine nucleotide exchange factor (GEF) that is known to be a regulator of actin cytoskeleton remodeling. Recently, a novel splicing isoform, βPix-b_L, was identified as an alternative translational product of the βPix-b mRNA with an extended N-terminus comprising a partial calponin homology (CH) domain and a serine-rich (SR) domain. However, the cellular function of βPix-b_L is largely unknown. In the current study, we analyzed the genomic DNA structure and cellular functions of βPix-b_L. The results of this study demonstrate that βPix is composed of 24 exons and 21 introns spanning around 100 kb. RT-PCR experiments revealed that there are two forms of βPix mRNA with distinct 5′ UTRs that are the result of alternative splicing of exon 1 and 2 from βPix genomic DNA. In addition, affinity chromatography analysis and a pull-down assay with the N-terminal region of βPix-b_L revealed that βPix-b_L interacts with tubulin and actin via its N-terminal CH and SR domains, respectively. Interaction with tubulin enabled βPix-b_L to bundle the microtubule and form membrane protrusions. Furthermore, the N-terminus of βPix-b_L was also critical for its localization to cellular vesicles. Functionally, βPix-b_L induced pinocytosis through cooperative action of the CH and Dbl homology (DH) domains, demonstrating the role of βPix-b_L in the regulation of membrane dynamics.

Keywords βPix · Pinocytosis · Calponin homology domain · Actin · Microtubule · Cell spreading

Seung Joon Lee and Soo Jung Yang have contributed equally to this work.

D. H. Kim · K. H. Lee · K. H. Choi · S. Rhee (✉)
Department of Life Science, College of Natural Sciences, Chung-Ang University, Seoul 156-756, Korea
e-mail: sangmyung.rhee@cau.ac.kr

S. J. Lee · S. J. Yang · D. Park
School of Biological Sciences, Seoul National University, Seoul 151-742, Korea

J. H. Pak
Asan Institute for Life Sciences, University of Ulsan College of Medicine, Asan Medical Center, Seoul 138-736, Korea

Present Address:
S. J. Lee
Nemours Center for Childhood Cancer Research, A. I. DuPont Hospital for Children, Wilmington, DE 19803, USA

Present Address:
S. J. Yang
Department of Molecular and Cell Biology, University of California, Berkeley, CA 94720, USA

Introduction

Two members of the Pix (p21-activated protein kinase (PAK)-interacting exchange factor) family, αPix (ARHGEF6) and βPix (ARHGEF7), have been identified as putative guanine nucleotide exchange factors for Rac/Cdc42, and as regulators of cytoskeleton remodeling/cell motility [1–3]. Recently, a novel βPix isoform, βPix-b_L, has been characterized as an alternative translational product from the βPix-b mRNA [4]. In comparison to βPix-b, βPix-b_L has an additional partial calponin homology (CH) domain and serine-rich (SR) domain in its N-terminus, which suggests distinct functions between these two isoforms. The CH domain is usually found in proteins that interact with actin filaments and microtubules [5, 6], and moreover, a mutation in the CH domain of αPix was identified in patients with X-linked, non-specific mental retardation [7], suggesting that βPix-b_L may be

involved in regulating cytoskeletal dynamics via its N-terminus.

βPix is known to play a role in cell migration by regulating the turnover of adhesions and remodeling of cytoskeletons through interactions with diverse signaling molecules including Rac1 and Pak1 [8]. Interestingly, several reports have suggested that microtubule growth induces activation of Rac1, which in turn modulates actin dynamics by inducing the formation of lamellipodia and membrane protrusions [9–12]. In contrast, the disassembly of microtubules results in activation of Rho, which enhances myosin contractility and stress fiber formation [13, 14]. These observations demonstrate that microtubule dynamics acts as one of the driving forces for cell migration through subsequent regulation of actin reorganization [15]. In addition to the regulation of actin/microtubule dynamics, rearrangement of the membrane through endocytosis is a key step in cell migration [16, 17]. However, relatively little is known about the functions of signaling molecules that link the signaling networks of endocytosis, cytoskeletal rearrangement, and activation of small GTPases.

In the current study, we show that βPix mRNA has two distinct 5′ UTR sequences as a result of alternative splicing of either exon 1 and 3 or exon 2 and 3, the latter encoding βPix-b_L. Biochemical analysis of the N-terminal region of βPix-b_L revealed an interaction with tubulin and actin directly through the partial CH and SR domains, respectively. Binding of βPix-b_L with tubulin led to stabilization of microtubules and subsequent membrane protrusion. Furthermore, overexpressed βPix-b_L increased cellular endocytosis through localization on cellular vesicles via the CH domain and activation of Rac/Cdc42 mediated by Dbl homology (DH) domains. These results suggest that βPix-b_L functions as a linker molecule coordinating pinocytosis and microtubule dynamics to regulate cell spreading and migration.

Materials and methods

Total RNA extraction and RT-PCR

Total RNA was extracted from mouse embryonic and adult brain cells using Trizol reagent according to the manufacturer's instructions (Invitrogen). First-strand cDNA was prepared from total RNA using oligo(dT)15 and SuperScript II (Invitrogen) following the manufacturer's protocol. PCR amplification was carried out using Ex-Taq DNA polymerase (Takara), according to the manufacturer's instructions. Oligonucleotide sequences of primers used in this study were as follows: forward primers 5′-GGACCC TGAGGTCTTCTTG-3′ for exon 1 and 5′-TAGGAAGGG GAGCGGATGAA-3′ for exon 2; reverse primer 5′-CTT CCTCACCAGCTTCTCTA-3′ for exon 23. The PCR products were resolved using 0.8% or 1.2% agarose gel electrophoresis and visualized with ethidium bromide staining.

Quantification of mRNA levels by real-time PCR

Total RNA was isolated using Trizol reagent, and the purified RNA was reverse transcribed with the iScript™ kit (Bio-Rad). Quantitative PCR analysis was performed with the ABI Prism 7900 Sequence detection system (ABI) using SYBR green PCR master mix (ABI). The relative expression of the investigated genes was quantified after normalization against β2-microglobulin. Primer sequences used for qPCR were as follows: β2-microglobulin forward primer 5′-TT CTGGTGCTTGTCTCACTGA-3′, reverse primer 5′-CAG TATGTTCGGCTTCCCATTC-3′; long UTR forward 5′-T TCTTGCAGGCGTCGCTCAAGG-3′ and reverse 5′-TGT TGCTCAGGCACTCGCTCTC-3′; Short UTR (for βPix-b_L) forward 5′-CTAGGAAGGGGAGCGGATGAA-3′ and reverse 5′-CCAAGGAGCTGAGGACCTTGT-3′.

Affinity chromatography

For purification of proteins bound to the N terminus of βPix-b_L, mouse brains were homogenized in homogenization buffer (10 mM Tris–HCl pH 7.4, 1 mM EDTA, 1 mM phenylmethylsulfonyl fluoride (PMSF), 1 mM leupeptin, 1 mM aprotinin). 260 mg of the resulting supernatant was then loaded onto a GST affinity column connected to a GST-N-terminus affinity column at a flow rate of 10 ml/h. The column was washed with washing buffer (10 mM KH_2PO_4 pH 7.4, 2 mM Mg acetate, 0.1 mM EGTA, 0.3 mM PMSF) five times, and the bead-bound proteins were eluted with elution buffer (20 mM glutathione, 120 mM NaCl, 100 mM Tris–HCl pH 8.0, 1 mM EDTA, 1 mM EGTA, and protease inhibitor cocktail). Aliquots of the bead-bound fractions were analyzed by 10% SDS-PAGE and silver staining and then compared to identify proteins that were present in the GST-N-terminus bead bound-fractions, but not in the GST bead bound-fractions. Bands corresponding to the major affinity-selected proteins were identified by matrix-assisted laser desorption ionization-time of flight (MALDI-TOF) mass spectrometry.

GST pull-down assay

For the pull-down assay, 1 mg of mouse brain lysate was incubated with GST or GST-fusion proteins in binding buffer (10 mM Hepes, pH 7.4, NaCl 150 mM, 0.5% NP-40, protease inhibitor cocktails) for 2 h at 4°C, followed by an additional incubation with Glutathione Sepharose (GE healthcare) for 2 h at 4°C. Binding proteins were subjected

to SDS-PAGE for immunoblotting with various antibodies. Proteins in the membrane were then visualized by treating with ECL reagent as recommended by the manufacturer.

Immunocytochemistry

Cells grown on 0.1% gelatin-coated coverslips were fixed for 10 min in 3.7% paraformaldehyde in phosphate-buffered saline (PBS), then permeabilized for 5 min with 0.5% Triton X-100 in PBS. Coverslips were blocked by incubating for 1 h in 10% goat serum and 0.1% gelatin containing PBS at room temperature. The cells were incubated with primary antibody for 1 h, washed three times with 0.1% Trion X-100 in PBS, and stained with fluorescein- or rhodamine-conjugated secondary antibodies (Jackson ImmunoResearch Laboratories, Inc.) for 45 min. Cells were observed under a fluorescence microscope (Axioplan2, Zeiss) equipped with a 63× (1.4 NA) Planapochromat objective lens or a Biorad confocal microscope (Radience 2000). Fluorescence images were collected using a cooled charge coupled-devised (CCD) digital camera (Axio-Cam, Zeiss).

Dextran uptake

Experiments for 70-kDa tetramethyl rhodamine isothiocyanate (TRITC)-conjugated-dextran (tDx) (Molecular Probes, Eugene, OR) uptake and quantification were performed as described previously [18]. Briefly, COS7 cells expressing vector, βPix-b_L, or truncated mutants were incubated with 0.5 mg/ml lysine fixable 70-kDa tDx for 10 min. After tDx uptake, the cells were fixed for 1 h in a modified periodate-lysine-paraformaldehyde fixative. Transfected cells were detected by staining with anti-Flag antibody. The relative level of tDx uptake scored as undetectable, moderate, or significantly enhanced dextran uptake was quantified with a fluorescence microscope as shown in the representative fluorescent micrographs. All graphs represent data obtained from three separate experiments.

Results

Analysis of alternative splicing in the βPix gene

βPix-b_L is one of the largest protein isoforms of βPix and it contains a partial CH domain in its N-terminus that is generated by alternative translational initiation at the 5′ UTR [4]. Recently, a novel clone related to βPix (Accession number: NM_001113517) was deposited, which may encode the complete CH domain, although its actual presence has not yet been validated. Comparison of the DNA sequence of βPix-b_L and this novel clone suggest possible alternative splicing in the 5′ region (Fig. 1a) that may enable the production of two distinct messages. Analysis of the mouse genomic DNA sequence of βPix revealed that the βPix gene is composed of 24 exons spanning more than 100 kb. Interestingly, we found evidence for possible alternative splicing of exon 1 and 2. While a transcript starting from exon 2 encodes βPix-b_L with a partial CH domain, another transcript that includes exon 1, but skips exon 2, would generate a second isoform with a full CH domain in the N-terminus. First, we examined the existence of these two messages resulting from alternative splicing at the 5′ UTR region by RT-PCR with RNA extracted from either adult or embryonic mouse brain cells (E18). Specific primers against exons 1 and 2 were used separately with a primer against exon 23 to amplify the entire structural region of the βPix-b protein. Both primer sets amplified specific bands with expected sizes (Fig. 1b), indicating the existence of two transcripts with different 5′ UTR sequences of the βPix-b gene in developing and adult mouse brain cells.

As shown in Fig. 1c, a second round of RT-PCR performed with the exon 2-specific primer pair failed to amplify any product when the PCR product generated with the exon 1-specific primer was used as a template. This result clearly showed the existence of alternatively spliced isoforms containing either exons 1 and 3 or exons 2 and 3, the latter encoding βPix-b_L mRNA.

Since the expression level of βPix-b_L was high in the embryonic stage during brain development [4], we tested to determine if the expression levels of these two transcripts are controlled differently during brain development. Comparison of the relative level of each transcript from adult and embryonic stages by quantitative real-time PCR indicated that the exon 2-containing mRNA (short 5′ UTR) encoding βPix-b_L is maintained at an almost similar level throughout development stages, whereas the mRNA with exon 1 (long 5′ UTR) was predominantly expressed in embryonic brains, suggesting that the expression of βPix-b_L might be tightly controlled by translational mechanisms rather than by transcriptional regulation [4].

Identification of binding proteins of the βPix-b_L N-terminus

As mentioned above, βPix-b_L contains partial CH and SR domains in its N-terminus. Therefore, we attempted to isolate N-terminus-interacting proteins of βPix-b_L to infer the cellular function of βPix-b_L. Interacting proteins were purified from mouse brain lysates using GST-N-terminus affinity column chromatography and identified by MALDI-TOF

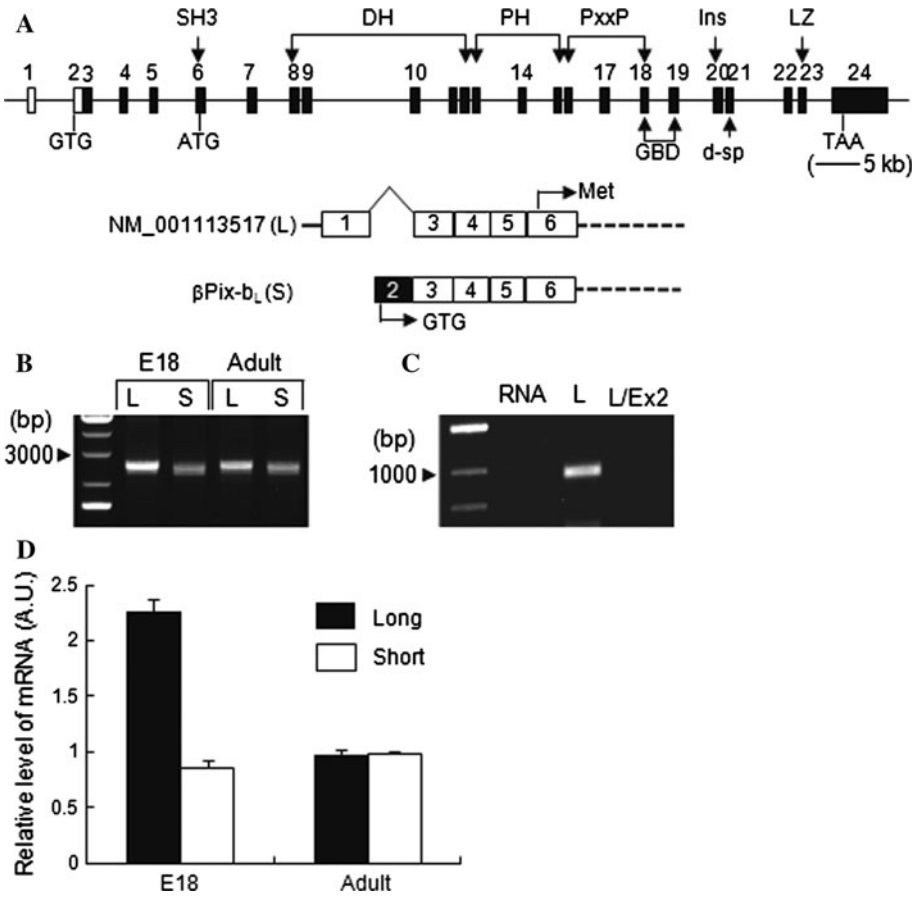

Fig. 1 Alternative splicing of βPix 5′ UTR. **a** Schematic presentation of the βPix genomic structure. Each exon is represented by a numerically labeled *black box* and sizes of the exons are not to actual scale. The schematic organization of the identified domains in the βPix protein is indicated by *arrows*. The putative alternative splicing in the 5′ UTR is shown with the two different transcripts depicted below. Exon 2, which is specific for βPix-b_L, is marked in black. **b** Analysis of transcripts containing exon 1 (L) and exon 2 (S) by RT-PCR. RT-PCR was carried out with mouse adult or 18 embryonic day (E18) brain total RNA using exon 1 or exon 2 primers paired with an exon 23 primer to amplify the entire ORF of βPix. **c** Second round RT-PCR from **b** shows that the exon 1 product (L) failed to amplify with the exon 2-specific primer (L/Ex2). **d** Relative quantities of transcripts containing exon 1 (L) and exon 2 (S) in embryonic and adult mouse brain cells. Averages of relative quantities of each transcript from 4 mice per group are shown. *Error bars* indicate standard deviations

mass spectrometry analysis (Fig. 2a). Several proteins, including tubulin β5 and α6 chain, interferon-induced RNA-activated protein kinase (PKR), and γ-actin were found to interact with the N-terminus of βPix-b_L. Western blot analysis with anti-βtubulin and anti-actin antibodies confirmed that the N-terminus of βPix-b_L specifically interacts with both β-tubulin and actin (data not shown).

To determine the specific region within the N-terminus of βPix-b_L that interacts with tubulin and actin, a series of GST-tagged deletion mutants of the N-terminus were tested for their ability to bind tubulin or actin. Pull-down analysis revealed that the CH domain interacts with tubulin, while the SR region is required for binding with actin (Fig. 2b, c). Interestingly, the isolated CH domain exhibited weaker binding affinity with tubulin than the whole N-terminus region, suggesting that the SR region may be needed in addition to the CH domain to increase the binding affinity of the N-terminus for microtubules. However, in the case of actin binding, the CH domain seems to be inhibitory as the isolated SR region exhibited enhanced affinity toward actin.

We then performed a microtubule co-sedimentation assay to further examine whether the N-terminus of βPix-b_L interacts directly with microtubules. Figure 2d shows that when GST-N-term is incubated with taxol-stabilized microtubules, most of the proteins were found in the microtubule-containing pellet fraction where the polymerized microtubules sediment. In contrast, GST or GST-SH3 protein was present only in the soluble fraction, which did not contain microtubules, clearly demonstrating that the N-terminus of βPix-b_L specifically and directly interacts with microtubules.

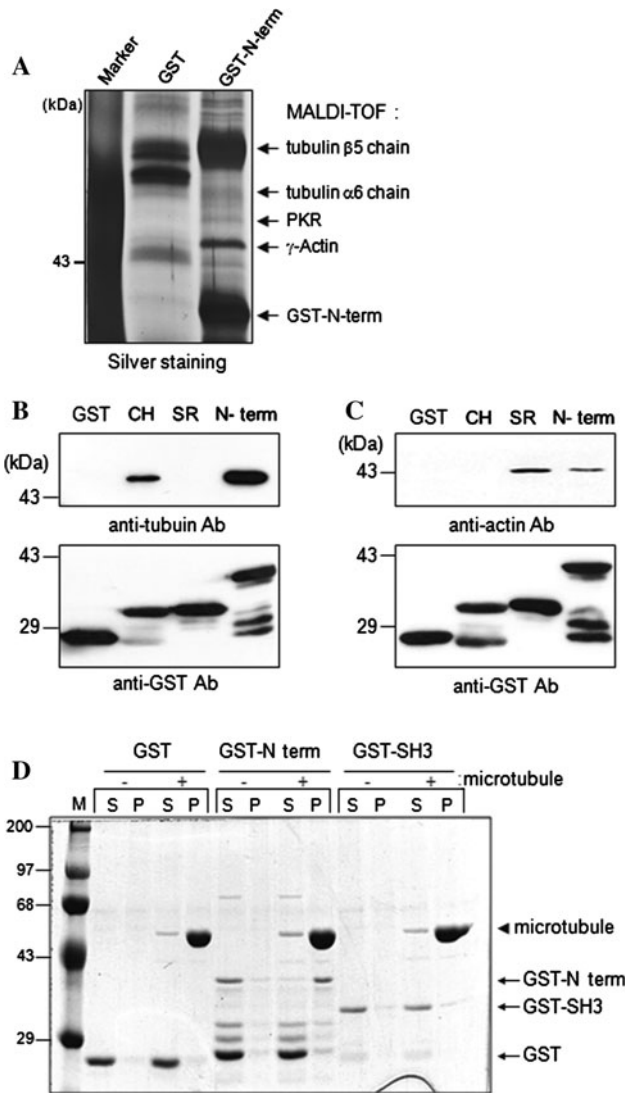

Fig. 2 Identification of βPix-b_L N-terminal binding proteins. **a** Silver-stained gel of the bead-bound fractions after chromatography of mouse brain lysates on Sepharose beads bound to the GST or GST-N-terminus containing the CH domain. The major affinity-selected proteins were analyzed by MALDI-TOF mass spectrometry. The results of the mass spectrometry are shown on the right. **b**, **c** Individual GST-fusion proteins were incubated with mouse brain lysates and the coprecipitating proteins were resolved on SDS-PAGE and analyzed with anti-tubulin (**b**) or anti-actin (**c**) antibodies. **d** Taxol-stabilized microtubules were incubated with the indicated GST-fusion proteins. They were allowed to bind for 30 min at 37°C. Microtubules were then pelleted by ultracentrifugation. Supernatants (S) and pellets (P) were subjected to SDS-PAGE. The *arrowheads* indicates sedimented microtubules, while *arrows* indicate GST, GST-SH3, or GST-N-terminus of βPix-b_L, respectively

Overexpression of βPix-b_L promotes membrane protrusion and cell spreading

To investigate whether βPix-b_L can affect membrane dynamics through binding to microtubules, we next analyzed the effect of βPix-b_L overexpression on cell spreading. Figure 3a shows the effects of wild-type βPix-b_L and CH domain-truncated constructs on cell spreading on fibronectin-coated coverslips. Cells expressing wild-type βPix-b_L exhibited formation of membrane protrusions enriched with microtubules, whereas cells overexpressing the CH domain-deficient mutant failed to form these dendritic protrusions. Morphometric analysis of a representative experiment showed that the projected area was much higher in βPix-b_L transfected cells (Fig. 3b), indicating that βPix-b_L plays a critical role in microtubule bundling and subsequently affects cell spreading.

Since microtubule stability can also induce microtubule bundling, we assessed the βPix-b_L-dependent formation of stable (nocodazole-resistant) microtubules. Figure 3c shows the typical microtubule structure of wild-type and truncated constructs of βPix-b_L-overexpressing cells upon nocodazole treatment, and Fig. 3d shows quantification of these results. A subpopulation of microtubules in βPix-b_L-overexpressing cells became nocodazole-resistant, whereas such a phenotype was not observed in cells expressing the CH domain alone or the CH domain-deleted mutant.

CH domain localizes βPix-b_L to pinocytic vesicles

From βPix-b_L overexpression experiments, we unexpectedly observed that βPix-b_L is distributed within the cell in vesicle-like structures (Fig. 3a). To examine which protein domain in βPix-b_L is responsible for targeting to these vesicles, various deletion and point mutants were generated as shown in Fig. 4a. As shown in Fig. 4b, wild-type βPix-b_L was localized to vesicular structures throughout the cytoplasm of transfected cells. These vesicles were smaller at the cell periphery and gradually increased in size around the nucleus (βPix-b_L). βPix-b was also targeted to the vesicular structures, but the vesicles stained with βPix-b were relatively large and uniform in size, and also fewer in number (βPix-b).

The unique cellular localization of βPix-b_L seems to indicate that the N-terminus of βPix-b_L most likely plays a specific role in cellular localization. Thus, the next experiment was designed to determine whether this N-terminal sequence is responsible for the cellular distribution of βPix-b_L. Overexpression of isolated N-terminus amino acid, 1-105, of βPix-b_L was localized to vesicle structures. However, the vesicles were smaller and irregular in shape and displayed a random spotty distribution in the cytoplasm (Fig. 4b, N-term), indicating that other domains in βPix-b_L are necessary for either the fusion or development of the vesicles.

To further investigate which protein domains are required for βPix-b_L-mediated vesicle formation, we examined the effect of mutations in the CH, SH3, and DH domains on βPix-b_L-mediated vesicle formation. Deletion

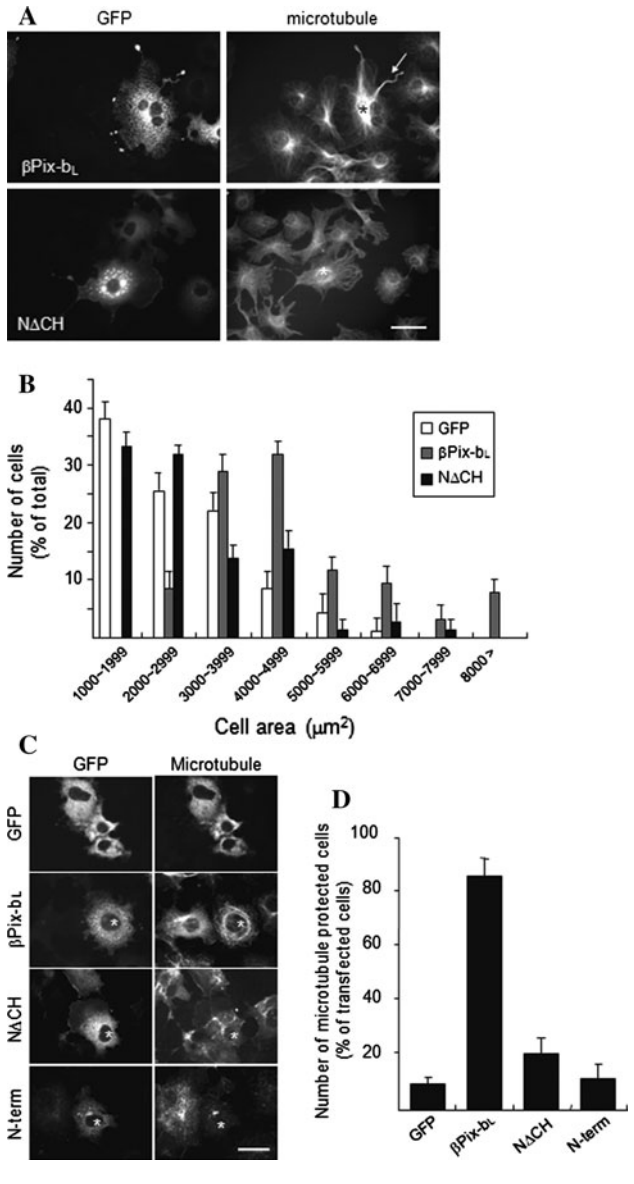

Fig. 3 Effect of βPix-b_L on microtubule-mediated cell spreading. **a** Cells were transfected with plasmids encoding either GFP-tagged βPix-b_L or N-terminus-truncated mutant (NΔCH) for 24 h and replated on fibronectin-coated coverslips for 12 h. Cells were fixed and stained with tubulin antibodies. Note the punctate expression of βPix-b_L throughout the cytoplasm. The *arrow* indicates the microtubule bundles that were present only in cells overexpressing βPix-b_L. Asterisks show transfected cells; *bar*, 20 μm. **b** Quantification of projected areas shown in **a**. Each value represents measurements made on 30–40 cells that were photographed at random. Values are mean ± S.D. for three separate experiments. **c** Cells were transfected with either GFP, βPix-b_L, N-terminal truncated mutant (NΔCH), or isolated N-terminus (N-term) for 24 h, after which the samples were treated with 1 μM nocodazole for 1 h, fixed with methanol (−20°C) for 10 min, then stained with anti-tubulin antibody. Stable microtubules were detected as previously described with minor modifications [35]. Asterisks indicate transfected cells; *bar*, 20 μm. **d** Quantification of nocodazole-resistant microtubules shown in **c**. Each value represents measurements from 30 to 40 cells in each experiment that were photographed at random. Values are mean ± S.D. for three separate experiments

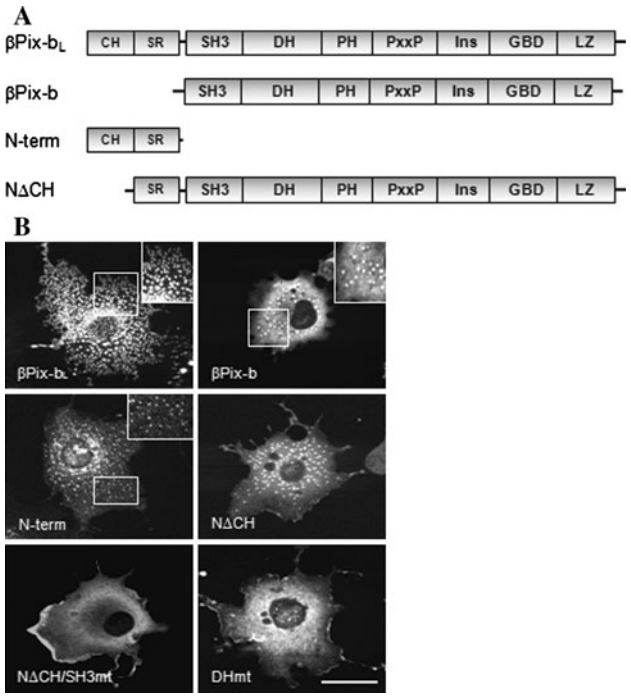

Fig. 4 Subcellular Distribution of βPix-b_L. **a** Diagram depicting the domain structures of βPix-b_L and the truncated constructs used for transfection experiments. Abbreviations: *LZ* leucine zip domain, *SR* serine rich domain, *SH3* Src homology 3 domain, *PH* pleckstrin homology domain, *PxxP* proline rich domain, *Ins* insert domain, *GBD* GIT binding domain. All constructs were tagged with Flag at their amino terminus. **b** Confocal images of COS7 cells expressing the indicated constructs. The subcellular distribution of the constructs was analyzed by immunostaining with anti-Flag antibody. *Insets* show enlargements of the marked areas; *bar*, 30 μm

of 35 amino acid residues in the N-terminus of βPix-b_L greatly impaired vesicle formation (Fig. 4b, NΔCH), and a mutant harboring double mutations in both the CH and SH3 domain exhibited complete loss of vesicle structures (Fig. 4b, NΔCH/SH3mt), indicating that the SH3 domain of βPix-b_L also plays a role in vesicle formation. Interestingly, most cells expressing NΔCH or NΔCH/SH3mt exhibited multiple protrusions and enhanced membrane ruffles. The DH domain mutant also exhibited complete loss of vesicle staining (Fig. 4b, DHmt) indicating that Rac activity through βPix-b_L is a prerequisite for vesicle formation or targeting.

Numerous studies have indicated that downstream effectors of βPix such as Rac and PAK are critical in macropinocytosis [18–22]. Therefore, we examined whether the βPix-b_L targeted vesicles are related to pinocytosis. When COS7 cells were allowed to take up 70-kDa Dextran-TRITC (tDx), a marker for fluid phase uptake [18], the tDx signal in the βPix-b_L overexpressing cells significantly colocalized with βPix-b_L-targeted vesicles as well as its isolated N-terminus-targeted vesicles (Fig. 5a). These results indicate that the βPix-b_L localizes to pinocytic vesicles. In support of an

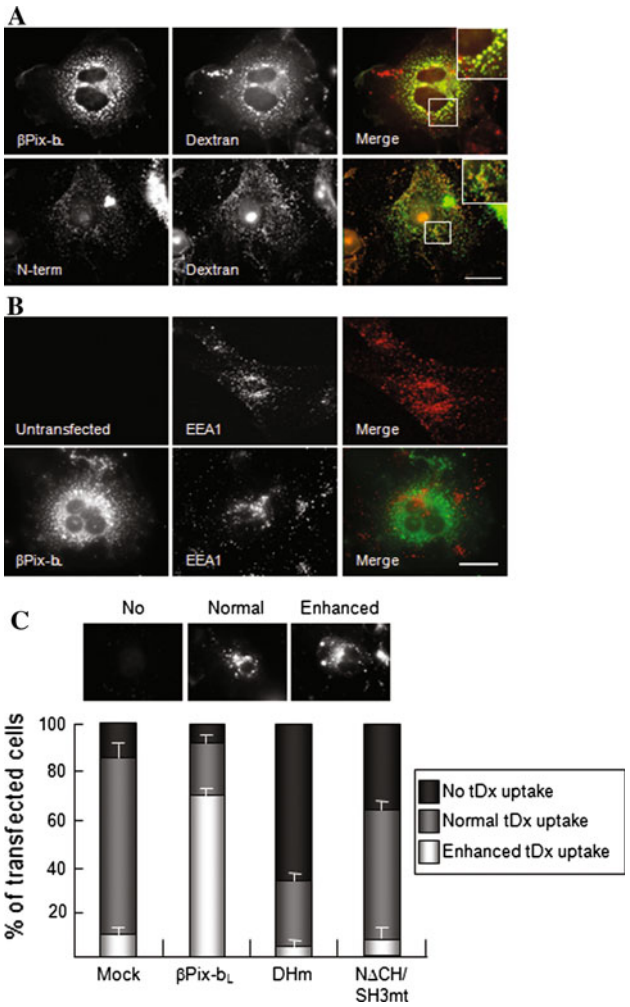

Fig. 5 βPix-b_L is localized to the pinocytic vesicles. **a** 0.5 mg/ml of lysine-fixable 70-kDa tDx was added to serum-starved COS7 cells expressing either flag-tagged βPix-b_L or isolated N-terminus (N-term), and then incubated for 10 min. Cells were fixed in a periodate-lysine-modified paraformaldehyde and stained with anti-Flag antibody, M2. Merged images show that either wild-type or N-terminus of βPix-bL-targeted vesicles were co-localized with Dextran-positive vesicles; *bar*, 20 μm. **b** EEA1-positive vesicles were visualized by immunostaining with anti-EEA1 antibody; *bar*, 20 μm. Note that no EEA-positive vesicles were co-localized with βPix-bL-targeted vesicles. **c** tDx uptake was measured in cells expressing wild-type or mutant βPix-b_L as explained in "Materials and methods" section. Cells were categorized as having "no", "normal" or "enhanced" tDx uptake according to the relative level of tDx uptake, as shown in the representative micrographs. A total of 50–70 transfected cells were counted for each condition in 10–12 separate fields. Results are given as percentages of cells in each category relative to the total number of cells counted. Values are mean ± S.D. for three separate experiments. Cells expressing βPix-b_L significantly increased tDx uptake

association of βPix-b_L with pinocytosis, neither the early endosome marker, EEA1-positive vesicles (Fig. 5b), nor the receptor-mediated endocytosis vesicles visualized by transferrin-FITC uptake (data not shown), overlapped with βPix-b_L-targeted vesicles.

Finally, we examined the effect of wild-type or various mutants of βPix-b_L on pinocytosis by assessing the uptake of tDx in COS7 cells. As shown in Fig. 5c, cells expressing βPix-b_L showed a ~50% increase in tDx uptake compared with mock-transfected cells. In contrast, expression of the DH mutant inhibited ~60% of tDx uptake as expected based on the essential role of Rac activation in initiating pinocytosis. The tDx uptake in cells expressing the NΔCH/SH3mt construct occurred to a similar extent as in the control cells.

Discussion

It has been reported that βPix-b_L can be synthesized by alternative translation using an unconventional GTG initiation site that results in an isoform containing a partial CH domain; however, another cDNA sequence (NM_001113517) related to βPix that was deposited in the NCBI database revealed that the 5′ UTR of the βPix gene can be subjected to alternative splicing using an additional exon. In the current study, we demonstrated that the transcript for βPix-b_L can be generated by the combination of exons 2 and 3 (Fig. 1a). We also found that transcripts for all the βPix isoforms reported to date can encode two transcripts by alternative splicing in the 5′ UTR (Fig. 1 and data not shown). The transcript of the βPix gene initiated with exon 1 possesses a putative translation initiation codon, AUG at position −84, instead of the GUG of βPix-b_L. Like βPix-b_L, in vitro expression of this transcript results in the production of two proteins, βPix-b and a larger size protein (unpublished data), but the amount of translated βPix-b is much lower compared to the amount of βPix-b_L. This seems to be due to the more efficient/dominant translational initiation from the AUG (exon 1) of this transcript in comparison to the GTG of βPix-b_L. Furthermore, quantitative real-time PCR results also demonstrate that the relative expression level of exon 2-containing transcript encoding βPix-b_L is relatively lower during brain development than the transcript consisting of exon 1, indicating that the expression of the βPix proteins could be regulated by differentially expressed splicing isoforms as well as alternative translation [4].

It is widely accepted that the Rho family GTPases and their downstream effectors are important regulators of macropinocytosis [19, 21, 23]. Our data show that SH3, DH, and CH protein domains in βPix-b_L act cooperatively to increase dextran uptake. One critical feature of βPix-b_L compared with other βPix isoforms is the presence of a partial CH domain in its N-terminus. It has been reported that the CH domain is responsible for directly linking signal transduction molecules via an association with cytoskeleton proteins [5, 6]. In the case of Vav, elimination

of the CH domain induces formation of depolymerization-resistant actin filaments and activates the transforming potential in NIH 3T3 cells, indicating that Vav is tightly regulated by actin binding through its CH domain [24]. Interestingly, deletion of the N-terminal 35 amino acids in βPix-b_L also facilitates actin binding and bundling of actin filaments (data not shown), suggesting the possibility that βPix-b_L may also regulate actin dynamics through its CH domain.

We also demonstrated another feature of the N-terminus of βPix-b_L: direct interaction with tubulin through its CH domain. It has been reported that several microtubule binding proteins, including EB1, were found to interact with tubulin through their CH domain [25–28]. In contrast to results for EB1, which interacts specifically to the tip of microtubule, we were unable to observe such localization of βPix-b_L. Instead, it was observed that βPix-b_L can bundle the microtubule, enhancing its stability against nocodazole. It has been reported that several microtubule-binding proteins contribute to microtubule stability. For example, X-PAK5 proteins, a subfamily of PAK, can stabilize microtubules due to their interaction with the kinase, and X-PAK5-bound microtubules are strongly resistant to nocodazole treatment [29, 30]. In our study, microtubules in cells expressing intact βPix-b_L showed increased resistance to nocodazole treatment, whereas the CH domain-deleted mutant was not able to protect against microtubule disruption. Furthermore, βPix-b_L-mediated tDx uptake was also completely inhibited by taxol treatment (data not shown), suggesting that regulation of microtubule dynamics by βPix-b_L may be important for cellular pinocytosis.

Although the precise role of pinocytosis in cell physiology is unclear, it is known that macropinocytosis provides a driving force in moving cells by regulating membrane flux in fibroblasts [31, 32]. Cell migration at the leading edge accompanies continuous remodeling of actin structures and re-sorting of internalized membranes [33]. Thus, it is obvious that the molecules responsible for the regulation of pinocytosis and actin dynamics are also indispensable for cell motility. Furthermore, we suggested in a previous report that βPix isoforms may regulate neural migration or neurite extension by locally regulating small GTPases [34]. These notions and our observations strongly support the possibility that βPix-b_L plays an important role in neural cell migration with pinocytosis during embryogenesis. Further studies to elucidate the molecular mechanisms of βPix-b_L-mediated pinocytosis should improve our understanding of cell migration.

In summary, we showed that the 5′ UTR of the βPix gene can be alternatively spliced to generate βPix-b_L. We also identified binding proteins that interact with the unique N-terminus of βPix-b_L, demonstrating that the partial CH domain directly interacts with tubulin, while the SR domain interacts with actin. Through these interactions, the N-terminus of βPix-b_L can contribute to microtubule stability and actin cytoskeleton remodeling. Functionally, βPix-b_L is able to induce cellular pinocytosis through the cooperative action of the CH and Dbl homology (DH) domains, indicating that βPix-b_L might be critical for increasing membrane dynamics through the regulation of pinocytosis, cell spreading, and membrane protrusion.

Acknowledgment This work was supported by National Research Foundation of Korean Grant funded by the Korean Government (KRF-2008-331-C00223) to S.R. It was also supported by grant M103KV010013-04K2201-01310 from BRC funded by the Korean Government to D.P.

References

1. Koh CG, Manser E, Zhao ZS, Ng CP, Lim L (2001) Beta1pix, the pak-interacting exchange factor, requires localization via a coiled-coil region to promote microvillus-like structures and membrane ruffles. J Cell Sci 114(Pt 23):4239–4251
2. Manser E, Loo TH, Koh CG, Zhao ZS, Chen XQ, Tan L, Tan I, Leung T, Lim L (1998) Pak kinases are directly coupled to the pix family of nucleotide exchange factors. Mol Cell 1(2):183–192
3. Oh WK, Yoo JC, Jo D, Song YH, Kim MG, Park D (1997) Cloning of a sh3 domain-containing proline-rich protein, p85spr, and its localization in focal adhesion. Biochem Biophys Res Commun 235(3):794–798
4. Rhee S, Yang SJ, Lee SJ, Park D (2004) βPix-b_L, a novel isoform of betapix, is generated by alternative translation. Biochem Biophys Res Commun 318(2):415–421
5. Mateer SC, Morris LE, Cromer DA, Bensenor LB, Bloom GS (2004) Actin filament binding by a monomeric iqgap1 fragment with a single calponin homology domain. Cell Motil Cytoskelet 58(4):231–241
6. Orlova A, Rybakova IN, Prochniewicz E, Thomas DD, Ervasti JM, Egelman EH (2001) Binding of dystrophin's tandem calponin homology domain to f-actin is modulated by actin's structure. Biophys J 80(4):1926–1931
7. Kutsche K, Yntema H, Brandt A, Jantke I, Nothwang HG, Orth U, Boavida MG, David D, Chelly J, Fryns JP, Moraine C, Ropers HH, Hamel BC, van Bokhoven H, Gal A (2000) Mutations in arhgef6, encoding a guanine nucleotide exchange factor for rho gtpases, in patients with x-linked mental retardation. Nat Genet 26(2):247–250
8. Liu F, Jia L, Thompson-Baine AM, Puglise JM, Ter Beest MB, Zegers MM (2010) Cadherins and pak1 control contact inhibition of proliferation by pak1-betapix-git complex-dependent regulation of cell-matrix signaling. Molecular and Cellular Biology 30(8):1971–1983
9. Waterman-Storer CM, Worthylake RA, Liu BP, Burridge K, Salmon ED (1999) Microtubule growth activates rac1 to promote lamellipodial protrusion in fibroblasts. Nat Cell Biol 1(1):45–50
10. Takahashi K, Suzuki K (2009) Membrane transport of wave2 and lamellipodia formation require pak1 that mediates phosphorylation and recruitment of stathmin/op18 to pak1-wave2-kinesin complex. Cell Signal 21(5):695–703
11. Zaoui K, Honore S, Isnardon D, Braguer D, Badache A (2008) Memo-rhoa-mdia1 signaling controls microtubules, the actin network, and adhesion site formation in migrating cells. J Cell Biol 183(3):401–408

12. Suzuki K, Takahashi K (2008) Regulation of lamellipodia formation and cell invasion by clip-170 in invasive human breast cancer cells. Biochem Biophys Res Commun 368(2):199–204
13. Chang YC, Nalbant P, Birkenfeld J, Chang ZF, Bokoch GM (2008) GEF-H1 couples nocodazole-induced microtubule disassembly to cell contractility via RhoA. Mol Biol Cell 19(5): 2147–2153
14. Rhee S, Jiang H, Ho CH, Grinnell F (2007) Microtubule function in fibroblast spreading is modulated according to the tension state of cell-matrix interactions. Proc Natl Acad Sci USA 104(13): 5425–5430
15. Wehrle-Haller B, Imhof BA (2003) Actin, microtubules and focal adhesion dynamics during cell migration. Int J Biochem Cell Biol 35(1):39–50
16. Hehnly H, Stamnes M (2007) Regulating cytoskeleton-based vesicle motility. FEBS Lett 581(11):2112–2118
17. Soldati T, Schliwa M (2006) Powering membrane traffic in endocytosis and recycling. Nat Rev 7(12):897–908
18. Dharmawardhane S, Schurmann A, Sells MA, Chernoff J, Schmid SL, Bokoch GM (2000) Regulation of macropinocytosis by p21-activated kinase-1. Mol Biol Cell 11(10):3341–3352
19. Fumoto S, Nishi J, Ishii H, Wang X, Miyamoto H, Yoshikawa N, Nakashima M, Nakamura J, Nishida K (2009) Rac-mediated macropinocytosis is a critical route for naked plasmid DNA transfer in mice. Mol Pharm 6(4):1170–1179
20. Bryant DM, Kerr MC, Hammond LA, Joseph SR, Mostov KE, Teasdale RD, Stow JL (2007) Egf induces macropinocytosis and snx1-modulated recycling of e-cadherin. J Cell Sci 120(Pt 10):1818–1828
21. West MA, Prescott AR, Eskelinen EL, Ridley AJ, Watts C (2000) Rac is required for constitutive macropinocytosis by dendritic cells but does not control its downregulation. Curr Biol 10(14):839–848
22. Dharmawardhane S, Sanders LC, Martin SS, Daniels RH, Bokoch GM (1997) Localization of p21-activated kinase 1 (pak1) to pinocytic vesicles and cortical actin structures in stimulated cells. J Cell Biol 138(6):1265–1278
23. Schlunck G, Damke H, Kiosses WB, Rusk N, Symons MH, Waterman-Storer CM, Schmid SL, Schwartz MA (2004) Modulation of rac localization and function by dynamin. Mol Biol Cell 15(1):256–267
24. Kranewitter WJ, Gimona M (1999) N-terminally truncated vav induces the formation of depolymerization-resistant actin filaments in nih 3t3 cells. FEBS Lett 455(1–2):123–129
25. Friedberg F, Rivero F (2009) Single and multiple ch (calponin homology) domain containing multidomain proteins in *Dictyostelium discoideum*: an inventory. Mol Biol Rep 37(6):2853–2862
26. Straube A, Merdes A (2007) Eb3 regulates microtubule dynamics at the cell cortex and is required for myoblast elongation and fusion. Curr Biol 17(15):1318–1325
27. Dougherty GW, Adler HJ, Rzadzinska A, Gimona M, Tomita Y, Lattig MC, Merritt RC Jr, Kachar B (2005) Clamp, a novel microtubule-associated protein with eb-type calponin homology. Cell Motil Cytoskelet 62(3):141–156
28. Bu W, Su LK (2003) Characterization of functional domains of human eb1 family proteins. J Biol Chem 278(50):49721–49731
29. Faure S, Cau J, de Santa Bar P, Bigou S, Ge Q, Delsert C, Morin N (2005) Xenopus p21-activated kinase 5 regulates blastomeres' adhesive properties during convergent extension movements. Dev Biol 277(2):472–492
30. Cau J, Faure S, Comps M, Delsert C, Morin N (2001) A novel p21-activated kinase binds the actin and microtubule networks and induces microtubule stabilization. J Cell Biol 155(6):1029–1042
31. Gao YS, Hubbert CC, Lu J, Lee YS, Lee JY, Yao TP (2007) Histone deacetylase 6 regulates growth factor-induced actin remodeling and endocytosis. Mol Cell Biol 27(24):8637–8647
32. Sharma M, Henderson BR (2007) Iq-domain gtpase-activating protein 1 regulates beta-catenin at membrane ruffles and its role in macropinocytosis of *n*-cadherin and adenomatous polyposis coli. J Biol Chem 282(11):8545–8556
33. Palamidessi A, Frittoli E, Garre M, Faretta M, Mione M, Testa I, Diaspro A, Lanzetti L, Scita G, Di Fiore PP (2008) Endocytic trafficking of rac is required for the spatial restriction of signaling in cell migration. Cell 134(1):135–147
34. Kim S, Kim T, Lee D, Park SH, Kim H, Park D (2000) Molecular cloning of neuronally expressed mouse betapix isoforms. Biochem Biophys Res Commun 272(3):721–725
35. Rhee S, Grinnell F (2006) P21-activated kinase 1: Convergence point in pdgf- and lpa-stimulated collagen matrix contraction by human fibroblasts. J Cell Biol 172(3):423–432